第 32 卷第 3 期 无 机 化 学 学 报 Vol.32 No.3
2016 年 3 月 CHINESE JOURNAL OF INORGANIC CHEMISTRY 508-516

共轭有机分子 BDOBC16 在硅烷化 SBA-15 孔内的组装及其发光性质

黎甜甜[1] 袁 苑[2] 周安南[1] 徐庆红*,[1]
([1]北京化工大学理学院,化工资源有效利用国家重点实验室,北京 100029)
([2]中国石油天然气股份有限公司石油化工研究院,北京 100089)

摘要:4,4′-(9-(正十六烷基)咔唑-3,6-取代)二(6-(4-二苯胺苯基)-2,2-二氟-1,3,2(2*H*)-二氧杂环己烷硼)(简称 BDOBC16)是一种含 β 二酮硼二氟取代基团的共轭有机发光分子,将其组装到 3-氨丙基三乙氧基硅烷(APTES)修饰的 SBA-15 孔道中。研究发现,BDOBC16 分子中的氟硼键未发生分解,且 BDOBC16 的发光性质发生了很大变化。客体 BDOBC16 本身在紫外光激发下发红光,而当其组装到硅烷化 SBA-15 孔道内后,BDOBC16 被紫外光激发后发绿光,且组装后 BDOBC16 发光强度增强了 75 倍。研究结果表明,主客体分子之间的较强氢键作用是客体分子组装前后发光强度发生巨大变化的主要原因;另外,客体分子的高度分散有利于 BDOBC16 发光强度的提高,客体分子集聚对其发光有严重的淬灭作用。

关键词:共轭;介孔材料;硅酸盐;自组装;发光
中图分类号:O614 **文献识别码**:A **文章编号**:1001-4861(2016)03-0508-09
DOI:10.11862/CJIC.2016.067

A π-Conjugated Organic Molecule: BDOBC16 Assembly in Silylated SBA-15 and Luminescent Properties

LI Tian-Tian[1] YUAN Yuan[2] ZHOU An-Nan[1] XU Qing-Hong*,[1]
([1]*State Key Laboratory of Chemical Resource Engineering, Beijing University of Chemical Technology, Beijing* 100029, *China*)
([2]*Petrochemical Research Institute, PetroChina Company Limited, Beijing* 100083, *China*)

Abstract: 4, 4-(9-(*n*-Hexadecyl)carbazole-3,6-diyl)di(6-(4-(diphenylamino)phenyl)-2, 2-difluoro-1, 3, 2(2*H*)-dioxaborine) (named as BDOBC16), a kind of π-conjugated organic molecule containing β-diketone-boron difluoride groups, was assembled in SBA-15 modified with (3-aminopropyl)triethoxysilane (APTES), and fluorine-boron groups in molecule of BDOBC16 was found to be remained in the assembly. Results indicate that the organic compound in silylated SBA-15 emits green light while itself emits red light. The energy of 0.45 eV is found changeable in emission of the guest before and after assembly, and luminescent intensity of BDOBC16 increases 75 times after it was assembled. Strong H-bond existed between the host and the guest, which is regarded as main reason to result tremendous change in luminescence of the guest. Molecular aggregation is also found harmful while high dispersion is benefit to luminescence of the guest.

Keywords: conjugation; mesoporous material; silicates; self-assembly; luminescence

π-conjugated organic systems have attracted increasing attention in recent years due to their promising applications in sustainable and low-cost optoelectronic devices such as organic light emitting diodes (OLEDs), organic field effect transistors (OFETs) and organic photovoltaic cells (OPVs)[1-7].

收稿日期:2015-09-13。收修改稿日期:2016-01-14。
国家自然科学基金(No.U1362113)资助项目。
*通信联系人。E-mail:xuqh@mail.buct.edu.cn,Tel:010-64425385

Particularly, research on π-conjugated organic molecules emitting fluorescence under UV irradiation becomes an important area[8]. Numerous π-conjugated organic molecules have absorption in visible region because of decreasing on energy gap of π-π*, and they sometimes possess high energy quantum efficiency[9-10]. Most organic luminescent molecules exhibit strong luminescence in dilute solutions, but their luminescent intensities decrease greatly in improper solvent or in their solid state because of strong intermolecular π-π stacking interactions and non-radiative decay in the aggregations, which is called aggregation-caused quenching (ACQ)[11]. The ACQ effect, resulting in dissatisfactory efficiency of organic luminescent materials in the solid state, has become an obstacle to fabricate efficient light-emitting devices, for the materials must be fabricated in a solid state[12-14].

The host-guest chemistry, studied for near half century, provides an effective method to solve the problems[15-17]. Host-guest system has gained considerable interest for its superiority to prepare functional groups in a well-defined geometry[18], and it provides controllable possibility over interactions among the functional groups to obtain particular properties[19,20]. In case of inorganic zeolite-based host-guest system, the organic molecules with functional groups are assembled by gas diffusion or in solution state[21]. Interaction between the host and guest involves more than one type of noncovalent interactions, such as hydrogen bonding, hydrophobic association, electrostatic interactions, van der Waals forces, and π-π stacking[22]. Most of the hosts possess the groups mainly used as hinges like -NH_2 to connect organic panel units, which can form a variety of nanoscale architectures[23]. Some conjugated systems were assembled as components of the panel units for their interesting physical phenomena, such as optoelectronic properties[24].

Here a kind of rigid organic molecule with π-conjugated structure BDOBC16[7], was synthesized according to the reference[7]. The molecule has novel fluorineboron groups, which brings excellent fluorescent properties to the material[5,25]. However, low fluorescence-emission is found in its solid state for molecular aggregation. To conquer the flaws, BDOBC16 was assembled into the cavity of SBA-15 modified with (3-aminopropyl)triethoxysilane. Fluorineboron groups in molecule of BDOBC16 were found to be remained and H-bonds were formed between the guest and host, for the existence of amine groups in inner wall of the silylated mesoporous material and atom of F in BDOBC16[26]. Results indicate that the organic compound in silylated SBA-15 emits green light while itself emits red light, 0.45 eV energy is found changeable in emission of the guest before and after assembly, and luminescent intensity of BDOBC16 increases 75 times after it was assembled. Strong H-bonds between the host and guest is regarded as a main reason to result in tremendous change on luminescence of the guest.

1 Experimental

1.1 Materials

All chemicals used are of analytical reagent grade available from a commercial supplier without further purification. Tetraethoxysilane (TEOS, ≥99%) was obtained from Sinopharm Chemical Reagent Company (in Shanghai, PR China). (3-aminopropyl) triethoxysilane, ≥99%) was obtained from Sigma-Aldrich Company (a USA chemical company). The other reagents were obtained from Beijing Chemical Reagent Company (PR China).

All the solvents were dehydrated before used.

1.2 Synthesis of SBA-15

SBA-15 was synthesized according to the reference[27]. TEM images of SBA-15 longitudinal section and cross section are shown in Fig.1[28].

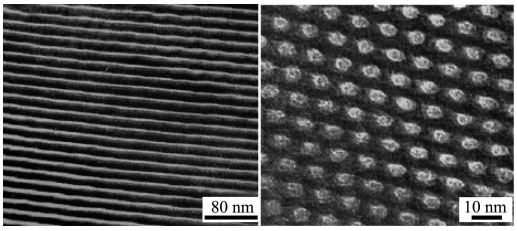

Fig.1　TEM images of SBA-15 cross section and longitudinal section

1.3 Synthesis of BDOBC16

BDOBC16, with molecular structure shown in

Scheme 1, was synthesized according to the method in the reference[7]. ^{1}H NMR (500 MHz, $CDCl_3$) δ: 8.45 (s, 2H), 8.03 (d, J=9.0 Hz, 2H), 7.98 (d, J=8.5 Hz, 4H), 7.37 (t, J=8.0 Hz, J=8.0 Hz, 8H), 7.32 (d, J=9.0 Hz, 2H), 7.25~7.18 (m, 12H), 7.03 (s, 2H), 6.98 (d, J=9.0 Hz, 4H), 4.22 (t, J=6.5 Hz, J=7.0 Hz, 2H), 1.86~1.81 (m, 2H), 1.31~1.21 (m, 26H), 0.86 (t, J=6.5 Hz, J=7.0 Hz, 3H). ^{13}C NMR (125 MHz, $CDCl_3$) δ: 179.9, 179.5, 154.3, 145.9, 144.9, 131.3, 130.3, 127.6, 127.0, 126.2, 124.5, 123.2, 123.1, 122.0, 118.9, 110.1, 92.0, 68.4, 44.2, 32.3, 30.1, 30.0, 29.9, 29.8, 29.7, 29.4, 27.6, 26.0, 23.1, 14.5. Elemental analysis for $C_{70}H_{69}B_2F_4N_3O_4$. Calcd (%): C, 75.48; H, 6.24; N, 3.77; Found:(%) C, 75.31; H, 6.12; N, 3.69.

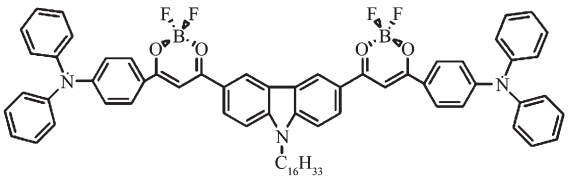

Scheme 1 Molecular structure of BDOBC16

1.4 Preparation of silylated SBA-15

0.5 g of dried SBA-15 was added into a 100.0 mL three-necked dried flask filled with N_2 gas. A solution of APTES (5.0 mL of APTES in 20.0 mL dried toluene) was added into the flask containing SBA-15 drop by drop. The mixture was stirred and refluxed at 90 ℃ for 16 h under protection of nitrogen gas. The final product was obtained by centrifugation, washed with chloroform, and dried at room temperature, and the result indicates that the mass fraction of the incoming group containing NH_2 is about 16.9% . Schematic drawing of the silylated course to SBA-15 is shown in Scheme 2.

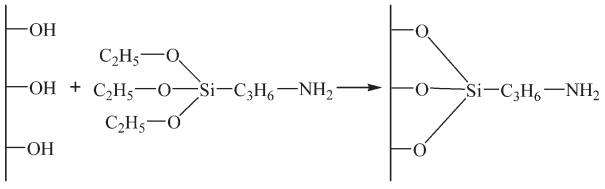

Scheme 2 Schematic drawing of the silylated course to SBA-15

1.5 Assembly of BDOBC16 into silylated SBA-15

0.1 g of silylated SBA-15 was added into a solution of BDOBC16 (0.01 g of BDOBC16 in 10.0 mL dried toluene). The mixture was stirred and heated at 60 ℃ for about 24 h. The assembly was obtained by centrifugation, washed with toluene and ethanol, and dried at room temperature. The mass percent of BDOBC16 in the assembly is about 15.5%.

1.6 Characterizations

Crystal structures of the samples were determined by powder X-ray diffraction (PXRD), using a Rigaku D/MAX diffractometer (made in Japan) with Cu $K\alpha$ radiation (λ=0.154 06 nm, scanning speed= 10°·min^{-1}). Solid-state ^{29}Si NMR spectra of the samples were obtained with a Bruker AV600 (made in Germany), and the chemical shifts recorded on the d-scale were referenced through external tetrakistrimethylsilane (TTMS). Fourier transform-infrared (FT-IR) spectra of the samples were recorded from KBr pellets (1 mg of sample to 100 mg of KBr) over the range of 400 ~ 4 000 cm^{-1}, at 2 cm^{-1} resolution using a Bruker Vector -22 spectrometer (made in Germany). UV-Vis spectra of the samples were performed in range of 200~600 cm^{-1} with a Perkin Elmer Lambda 900 UV-Vis spectrophotometer (made in Japan). N_2 sorption isotherms of the samples were recorded on a Quantachrome NOVA 2000e sorption analyzer (made in USA) at the temperature of liquid nitrogen (77 K). Samples were degassed at 200 ℃ overnight prior to the measurement. Surface area was obtained by Brunauer-Emmett-Teller (BET) method, and pore size distribution was calculated using Barret-Joyner-Halenda (BJH) model. Thermogravimetric analysis (TG) and differential thermal analysis (DTA) were performed on a HCT-2 thermoanalyzer (Beijing Hengjun Instrument Company) at a heating rate of 10 ℃·min^{-1}, raised from 25 to 800 ℃, using α-Al_2O_3 as the reference. X-ray photoelectron spectroscopic (XPS) analysis was measured on Shimadzu ESCA-250 and ESCA-1000 spectrometers (made in Japan) with Mg K X-ray sources. Emission spectra were collected on a Spex Fluorolog-7000 fluorimeter (made in Japan) with a 450 W Xe lamp as an excitation light source. The photoluminescence quantum yield and lifetime measurements were performed using a FLS-980 steady state and transient state fluorescence spectrometer made by Edinburgh

Instruments (UK).

2 Results and discussion

^{29}Si MAS NMR spectra of SBA-15 and the surface silylated SBA-15 sample are shown in Fig.2. The bands labeled Q2, Q3, and Q4 in Fig.2A correspond respectively to $(OH)_2Si(OSi)_2$, $(OH)Si(OSi)_3$, and $Si(OSi)_4$. After silylated, intensities of the relative peaks in the spectra are changed, indicating that silylation occurred during the treatment. The band assigned to $Si(OSi)_4$ increases in intensity (Fig.2B), proving the reaction between APTES and Si-OHs existing on the wall of SBA-15. The data of relative chemical shifts and some bands′ intensities are summarized in Table 1, and there is about 8.3% of the Si-OH groups in SBA-15 were silylated.

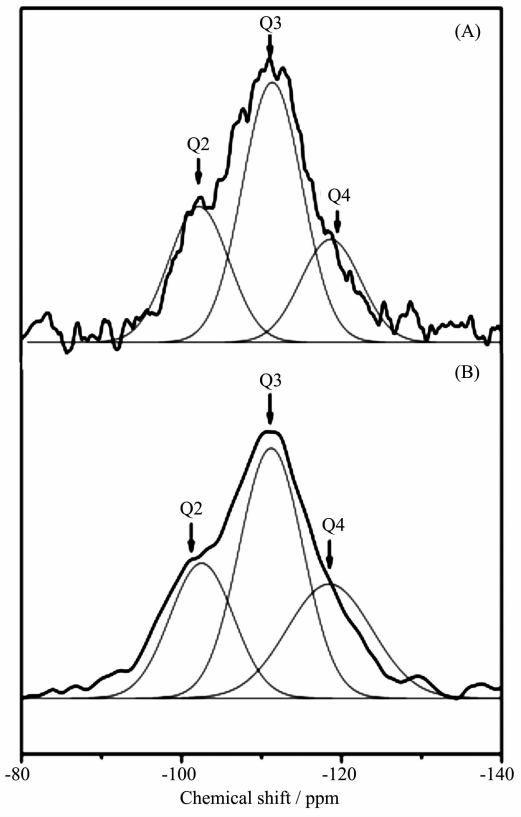

Fig.2　^{29}Si MAS NMR spectra of SBA-15 (A) and silylated SBA-15 (B)

The pore volumes and pore diameter distributions of SBA-15, silylated SBA-15 and the assembly (BDOBC16 in silylated SBA-15) were determined from N_2 adsorption isotherms at 77 K, which are shown in Fig.3. It can be easily found that the pore radius and pore volume decreased clearly from SBA-15 to the assembly, pore radius of silylated SBA-15 decreased from 3.268 to 2.462 nm after BDOBC16 assembled. TEM images (Fig.4) show that the diameters of silylated SBA-15 and the assembly all have some decrease, and the pores are obscure after BDOBC16 assembled.

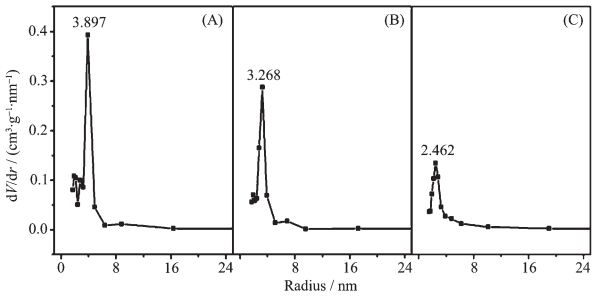

Fig.3　Pore size distributions for SBA-15 (A), silylated SBA-15 (B) and the assembly (C)

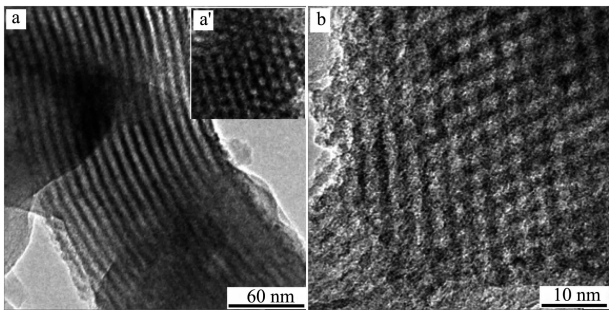

Fig.4　TEM images of silylated SBA-15 (a: longitudinal section; a′: cross section) and assembly (b: cross section)

FT-IR spectra of BDOBC16, SBA-15, silylated SBA-15, and the assembly are shown in Fig.5. In Fig. 5Aa, A broad peak at about 3 340 cm^{-1} are assigned as structural hydroxyl groups in the spectrum of dried SBA-15, which offers reactive resource to APTES. The

Table 1　^{29}Si MAS NMR data of SBA-15 and silylated SBA-15

Sample	Chemical shift			Intensity / %		
	Q2	Q3	Q4	Q2	Q3	Q4
calcined SBA-15	−102.5	−110.9	−118.5	27.4	52.2	20.4
APTES-SBA-15	−102.5	−111.2	−118.5	25.0	46.3	28.6

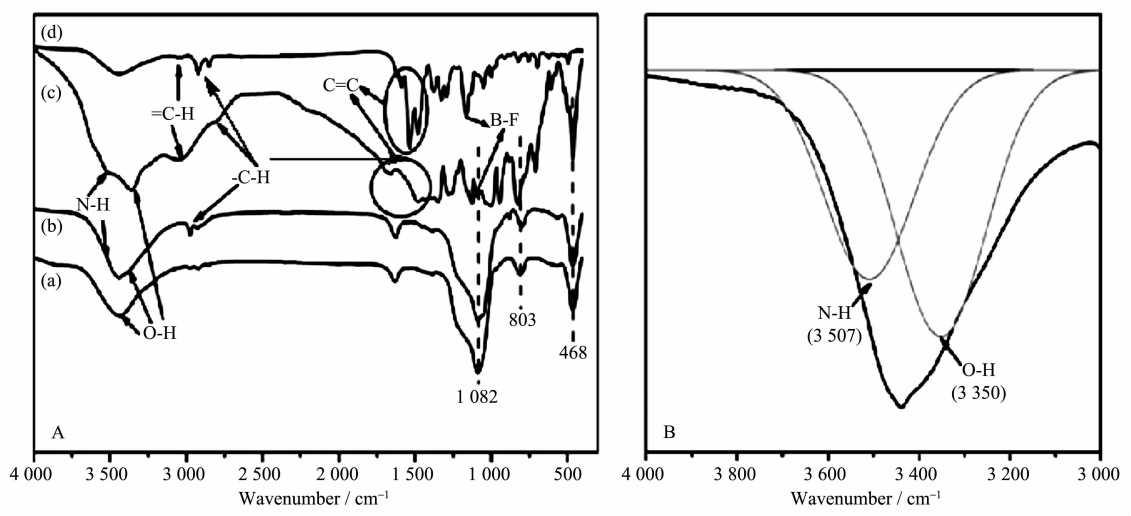

Fig.5 A: FT-IR spectra of dried SBA-15 (a), silylated SBA-15 (b), the assembly (c) and BDOBC16 (d); B: FT-IR spectra of silylated SBA-15 from 3 000 to 4 000 cm^{-1}

peaks at 1 082, 803, 468 cm^{-1} are attributed to asymmetric stretching, symmetric stretching and bending vibrations of Si-O-Si, respectively[28]. But in the spectrum of silylated SBA-15 (Fig.5Ab), the peak at 3 507 cm^{-1} contributed to N-H absorption (Fig.5B, amplified part from 3 000 to 4 000 cm^{-1} in silylated SBA-15) and the peak at 2 928 cm^{-1} contributed to C-H stretching absorptions from APTES are found. Compared to silylated SBA-15, absorption of N-H in the assembly (Fig.5Ac) has 8 cm^{-1} blue shift (from 3 507 to 3 515 cm^{-1}), indicating existence of H-bond between BDOBC16 and silylated SBA-15 possibly. Existence of H-bond also can be proved from the absorption shift of B-F bond in the assembly comparing to that of the absorption in BDOBC16. The absorptions of B-F bond in BDOBC16 and assembly are at 1161 (Fig.5Ad) and 1 135 cm^{-1} (Fig.5Ac)[29], respectively, 26 cm^{-1} blue shift happens. The other absorptions coming from the guest are all found in the assembly.

Presence of BDOBC16 in silylated SBA-15 is also proved by TG-DTA analysis. TG spectra of SBA-15, silylated SBA-15 and the assembly are shown in Fig.6A. To SBA-15 (Fig.6Aa), there is only about 1.13% mass loss observed below 100 ℃, which comes from the evaporation of adsorbed water in cavities of the zeolite and some residue of the template. But to silylated SBA-15 (Fig.6Ab), total weight loss from the organic part is about 18.0%, some from evaporation of adsorbed organic solvents (25~150 ℃, about 1.5%) and some from decomposition of organic part connected (150~600 ℃, about 16.5%). Little water was found to be contained in the sample, for SBA-15 was dried at 100 ℃ under vacuum for about 2 h before modification.

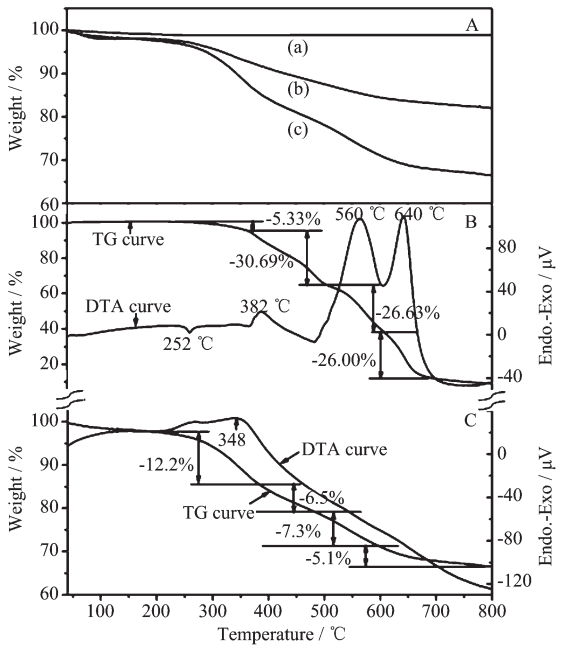

Fig.6 A: TG curves of SBA-15 (a), silylated SBA-15 (b) and the assembly (c); B: TG-DTA curves of BDOBC16; C: TG-DTA curves of the assembly

Figs.6B and 6C are the TG-DTA curves for BDOBC16 and the assembly, respectively. Weight loss of BDOBC16 is about 91.1% from 25 to 800 ℃ (Fig. 6B), which are divided into four steps. The first, from 180 to 360 ℃, is assigned to the loss of alkyl chain $C_{16}H_{33}$; The second, from 360 to 480 ℃, is inferred coming from decomposition of the triphenylamine groups; The third, from 480 to 600 ℃, possibly comes from the loss of carbazole groups; and the last, over 600 ℃, can be ascribed to decomposition of biphenyl in the center.

As to the assembly, five weight lost steps, corresponding to temperature changeable ranges 25~180 ℃ (evaporation of solvent), 180~380 ℃ (decomposition of aminopropyl connected with SBA-15 and alkyl chain $C_{16}H_{33}$), 380~490 ℃ (decomposition of triphenylamine groups), 490~600 ℃ (weight loss of carbazole groups) and over 600 ℃ (decomposition of biphenyl), are found in its TG analysis, and the total weight loss is about 33.5% (Fig.6C). Compared with silylated SBA-15, about 15.5% (33.5%-1.5%-16.5%) weight loss coming from the guest happens to the assembly. The last four weight loss steps of the assembly are well coincident with BDOBC16, and the temperature changeable ranges of BDOBC16 in the host are higher than that of the pure compound due to protection of the zeolite. Weight lost steps and their corresponding temperature changeable ranges to BDOBC16 and the assembly are listed in Table 2.

Compared to BDOBC16, number of exothermic peaks relating to the assembly decreases. One endothermic (at 252 ℃) and three exothermic peaks (at 382, 560 and 640 ℃, respectively) in TG curve are found relating to BDOBC16. However, only one exothermic peak at 348 ℃ involving the guest, no prominent peak over 450 ℃, is observed relating to the assembly. Some interactions, such as the hydrogen bonding, between silylated SBA-15 and the conjugated molecule possibly lead to the results.

UV-Vis absorption spectra of SBA-15, silylated SBA-15, assembly and BDOBC16 are shown in Fig. 7A. To BDOBC16, a broad absorption band from 290 to 350 nm, due to transitions of electrons in carbazole and triphenylaminecentered, is observed. Absorption bands form π-π* transition in the conjugated molecule are at 390 and 426 nm[7]. Moreover, the most interesting absorptions are charge transfers in the whole conjugated system, and two strong absorptions at 512 and 545 nm with high absorption coefficients might partly be ascribed to charge-transfer transitions. As to the assembly, the absorptions at 298 and 419 nm are from BDOBC16, and their positions in the conjugated molecule are at 304 and 426 nm, respectively. But the absorptions at 348 and 390 nm coming from carbazole group in BDOBC16 disappear and a new broad absorption band centered at 368 nm appears after the guest assembled, due to the influence from H-bond between the atoms of F in the guest and the imino groups existing on the surface of silylated SBA-15. The B element is electron deficiency,

Table 2　Weight loss steps and corresponding temperature change ranges of BDOBC16 and the assembly in their TG analysis

		BDOBC16	Assembly
Step 1	Weight loss / %	5.33	2.4
	Temperature range / ℃	180~370	25~180
Step 2	Weight loss / %	30.69	12.2
	Temperature range / ℃	370~490	180~380
Step 3	Weight loss / %	26.63	6.5
	Temperature range / ℃	490~600	380~490
Step 4	Weight loss / %	26	5.1
	Temperature range / ℃	600~680	490~600
Step 5	Weight loss / %		5.1
	Temperature range / ℃		600~800

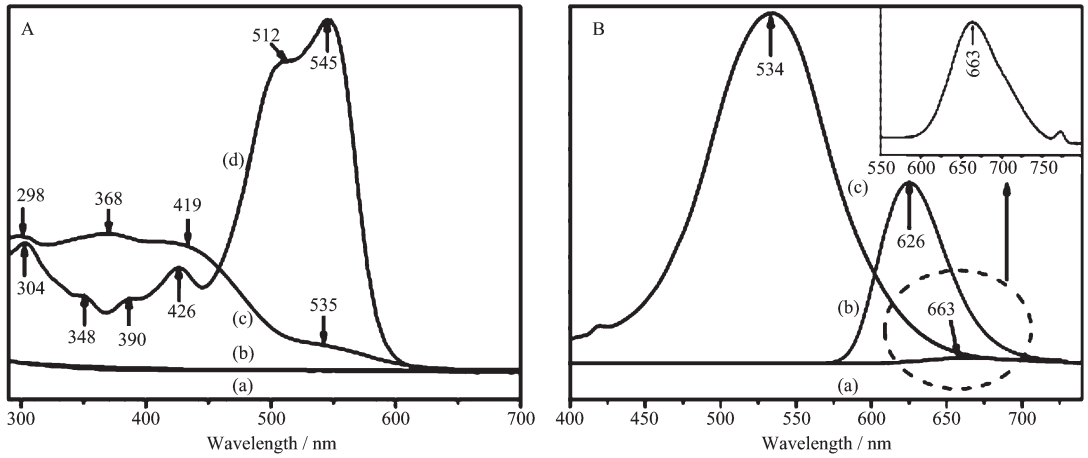

Fig.7 A: UV-Vis diffuse-reflectance spectra of SBA-15 (a), silylated SBA-15 (b), assembly (c) and BDOBC16 (d); B: fluorescence-emission spectra of solid BDOBC16 (a), BDOBC16 in toluene (10 μg·L^{-1}) (b) and the assembly (c)

and the BF_2 group is electrophilic forcefully. Before assembled, BDOBC16 has a typical D-Π-A-Π-D structure and strong intramolecular charge transfer property. Hydrogen bond between atom F (in BDOBC16) and NH_2 group (connected on the wall of silylated SBA-15) was possibly formed after formation of the assembly (Scheme 3). As it is known that the NH_2 group is a strong electron-donating group, the electronic receptive ability of BF_2 in BDOBC16 would be subdued greatly in the assembly. Thus, the original peak at 545 nm in the UV-Vis absorption spectra disappeared, and absorptions at 368 and 419 nm were observed.

The fluorescence emission spectra for BDOBC16 (solid), its solution (10 μg·L^{-1}) in toluene and the assembly are displayed in Fig.7B. The emission peak can be observed at 663 (Fig.7Ba, its amplified figure is shown in the upright) and 626 nm (Fig.7Bb) with area of 244.5 and 5 486 for BDOBC16 and its solution in toluene, respectively. The blue-shift for BDOBC16 in two states can be attributed to π-π^* or dipole-dipole interaction of the conjugated BDOBC16 molecules[7]. Moreover, a broad emission peak of the assembly is observed at 534 nm with area of 18 381.4 (Fig.7Bc). There is about 129 nm blue shift happening from red to green glow area and the luminescent intensity of BDOBC16 increases about 75 times before and after assembling, considering mass percent of the guest in host is about 15%. Some information about emission peaks of BDOBC16 and the assembly are listed in Table 3.

Table 3 Information about emission peaks of BDOBC16 and Assembly

Material and State	λ_{em} / nm	Area
BDOBC16 (solid)	663	244.5
BDOBC16 (dissolved in toluene)	626	5 486
Assembly	534	18 381.4

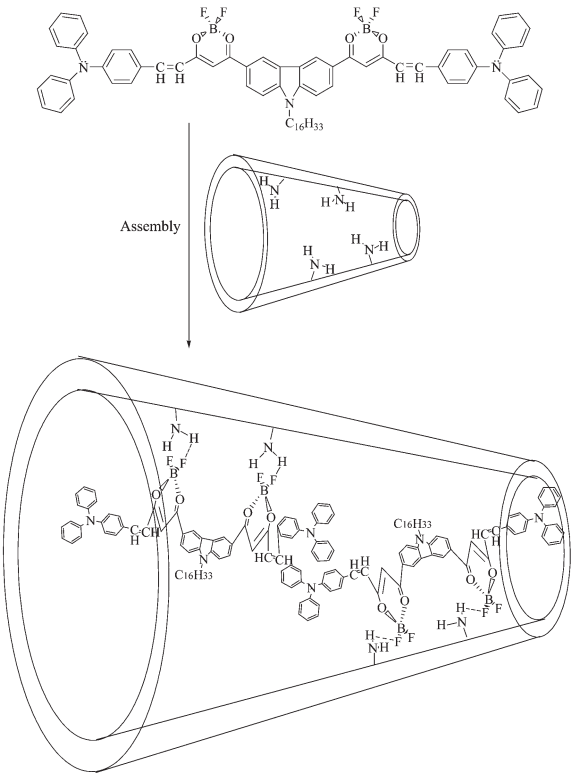

Scheme 3 Schematic drawing to the formation of assembly

The luminescent intensities of solid BDOBC16 and that of the organic compound in solution state are only about 1.3% and 29.8% to the assembly, indicating that the guest molecule dispersion affects its photoemission greatly. Energy quenching effect plays a leading role when the emitter molecules gather with each other, for the energy is transferred among the conjugate structures and consumed gradually. But in the assembly, the molecules of BDOBC16 are stabled by H-bonds in different wall surface positions of silylated SBA-15, energy quenching effect among the guest molecules disappears and its luminescent intensity is increased greatly.

Blue shift on emission wavelength of guest in silylated SBA-15 can be explained. As discussed above, strength of electron acceptor in BDOBC16 was greatly weakened due to the existence of the hydrogen bonds between F atoms (in BDOBC16) and NH_2 groups (connected on the wall of silylated SBA-15). That is to say, a higher energy is needed to excite the electron in BDOBC16 from a low energy level to a high energy lever. So the emission wavelength of the assembly has been blue shifted, and the fluorescence color of BDOBC16 changed from red to green after assembled.

To the original conjugate compound, electrons in π orbit jump from S_0 (the molecular ground state) to S_1 orbit (the first excited electronic singlet) after they are excited by UV light. But in silylated SBA-15, the π electrons in BDOBC16 are excited and possibly jump to S_2 orbit (the second excited electronic singlet), for the energy consumed in molecular vibration and motion is decreased greatly. Energy difference in two kinds of jumping for one electron is about 0.45 eV, which is calculated based on the equation of $E=hc/\lambda$, (where h is Planck constant, c is velocity of light and λ is the wave number of emission light). In this research, λ_1 is 626 nm and λ_2 is 534 nm, $\Delta E=hc\ (1/\lambda_2-1/\lambda_1)=6.626\times10^{-34}\ \mathrm{J\cdot s}\times3.0\times10^{8}\ \mathrm{m\cdot s^{-1}}\times(1/534-1/663)\ \mathrm{nm^{-1}}\times10^{9}/(1.6\times10^{-19}\ \mathrm{J\cdot eV^{-1}})=0.45$ eV.

Measurement shows that the fluorescent lifetime and quantum yield of BDOBC16 in silylated SBA-15 are 1.13 ns and 3.23%, respectively. Colours of the relative materials under UV (365 nm) and sun light irradiated are shown in Fig.8.

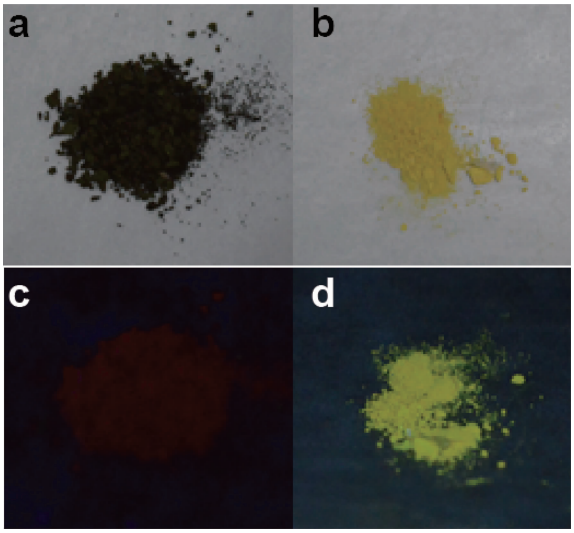

a and c come from BDOBC16, b and d come from the assembly

Fig.8　Colours of BDOBC16 and assembly under sun light (a and b) and UV light (c and d)

Existence of H-bonds between the guest and host is proved by XPS analysis to F1*s* and B1*s*. As shown in Fig.9, binding energy (BE) of F1s in F-B bond in BDOBC16 is about 686.5 eV (Fig.9A). However in the assembly, BE of F1*s* divides into two states, which locates at 685.3 and 688 eV (Fig.9B), respectively. The interaction between F atoms and silylated SBA-15 results in the change. Associating with molecular structure of BDOBC16, the interaction should come from the H-bonds between F atoms and -NH_2 groups. However the H-bond (B–F⋯H) possibly happens to

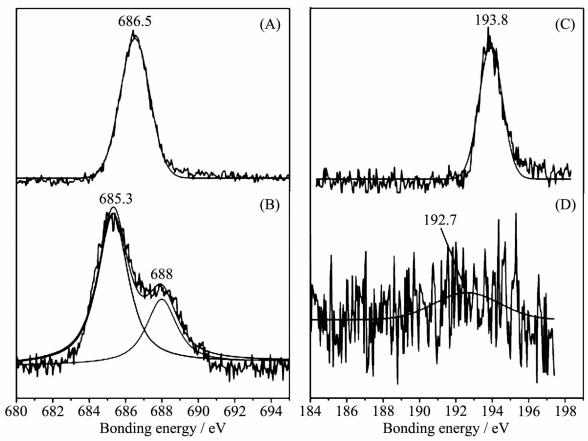

Fig.9　XPS spectra of F1*s* in BDOBC16 (A), assembly (B); XPS spectra of B1*s* in BDOBC16 (C) and the assembly (D)

one B-F bond and it makes that the other F atom bonding with the same B is different. Moreover, BE of the B atoms in BDOBC16 and in assembly are all found (shown in Fig.9C and 9D), proving the conjugated molecule was not damaged undergoing assembly. BE of B1*s* in BDOBC16 is about 193.8 eV, and it is about 192.7 eV in the assembly. 1.1 eV binding energy decreased in the two states indicates that the atoms of B in BDOBC16 are also suffered by H-bonds, which exists between F atoms and -NH_2 groups. If parts of BDOBC16 molecules are decomposed during the assembling, there should exist two states of B atoms in the assembly.

3 Conclusions

In summary, Bis(dioxaborine)carbazole derivatives (BDOBC16), a kind of π-conjugated organic luminophor molecule containing β-diketone-boron difluoride groups, was assembled in silylated SBA-15. XPS analysis indicates that the molecular structure of BDOBC16 was remained in the host, and there exist H-bond between the guest and host. Under UV irradiation, BDOBC16 emits green light after it was assembled in silylated SBA-15, while itself emits red light. Luminescent intensity of BDOBC16 increases 75 times after it was assembled. π electrons in the conjugate structure in silylated SBA-15 was found to be excited more effectively under UV light.

Acknowledgments: We are grateful to the financial support from Project of National Natural Science Foundation of China (Project No.U1362113), and the financial support from Petro China Company Limited.

References:

[1] Saito K, Kuwabara J, Kanbara T. *Synth. Met.*, **2011**,**161**: 1150-1153

[2] Park Y, Advincula R C. *Chem. Mater.*, **2011**,**23**:4273-4294

[3] Cai J, Niu H, Wang C, et al. *Electrochim. Acta*, **2012**,**76**: 229-241

[4] Rochat S, Swager T M. *ACS Appl. Mater. Interfaces*, **2013**,**5**: 4488-4502

[5] Zhou Y, Kim J W, Yoon J. *Organ. Lett.*, **2010**,**12**:1272-1275

[6] Ripaud E, Demeter D, Leriche P, et al. *Dyes Pigm.*, **2012**, **95**:126-133

[7] Liu X, Zhang X, Lu R. *J. Mater. Chem.*, **2011**,**21**:8756-8765

[8] Elson E L. *Biophys. J.*, **2011**:2855-2870

[9] Zhao C H, Wakamiya A, Inukai Y, et al. *J. Am. Chem. Soc.*, **2006**,**128**:15934-15935

[10]Li W, Li Q, Huang L Y F. *Dyes Pigm.*, **2015**,**113**:1-7

[11]Thomas III S W, Joly G D, Swager T M. *Chem. Rev.*, **2007**, **107**:1339-1386

[12]Zhao Z, Lu P, Tang B Z. *Chem. Sci.*, **2011**,**2**:672-675

[13]Chiang C L, Chen C T, Hsu C P, et al. *Adv. Funct. Mater.*, **2008**,**18**:248-257

[14]Liu J, Lam J W Y, Tang B Z. *Chem. Rev.*, **2009**,**109**:5799-5867

[15]Fan H, Hu Q D, Xu F J, et al. *Biomaterials*, **2012**,**33**:1428-1436

[16]Fujita M, Tominaga M, Hori A, et al. *Acc. Chem. Res.*, **2005**,**38**:369-378

[17]Shi W J, Menting R, Ng D K P. *Chem. Commun.*, **2013**,**49**: 5277

[18]Muraoka T, Kinbara K, Aida T. *Nature*, **2006**:440

[19]Wang L, Lei J, Ma R, et al. *Anal. Chem.*, **2013**,**85**:6505-6510

[20]Agasti S S, Liong M, Lee H, et al. *Angew. Chem. Int. Ed.*, **2012**,**51**:450-454

[21]Hu J, Liu S. *Chem. Mater.*, **2011**,**23**:1088-1090

[22]Hu J, Liu S. *Acc. Chem. Res.*, **2014**,**47**:2084-2095

[23]Chan M Y, Lai S L, Lee C S. *Adv. Funct. Mater.*, **2007**,**17**: 2509-2514

[24]Schenning A P H J, Meijer E W. *Chem. Commun.*, **2005**: 3245

[25]Zhou Y, Xiao Y, Li D, et al. *J. Org. Chem.*, **2008**,**73**:1571-1574

[26]Nandi M, Mondal J, Yamauchic Y, et al. *Chem. Commun.*, **2011**,**47**:6677-6679

[27]Zhao D Y, Feng J L, Huo Q, et al. *Science*, **1998**,**279**:548

[28]Zhao D Y, Yang P D, Melosh N, et al. *Adv. Mater.*, **1998**,**10** (16):1380-1385

[29]Mondal J, Borah P, Bhaumik A. *Org. Process Res. Dev.*, **2014**,**18**:257-265

[30]Ma R Z, Yao Q C, Yang X, et al. *J. Fluorine Chem.*, **2012**, **137**:93-98

[31]Xu Q, Li L, Liu X, et al. *Chem. Mater.*, **2002**,**14**(2):549-555